Dynamic Response Control of Linear Viscoelastic Materials as Resonant Composite Rheological Models

Polidor BRATU
The Institute of Solid Mechanics of the Romanian Academy, 15 Constantin Mille Str., 010141 Bucharest, Romania, bratupolidor@yahoo.com

Cornelia DOBRESCU
Faculty of Engineering and Agronomy in Braila, "Dunărea de Jos" University of Galati, 800008 Galati, Romania, cornelia.dobrescu@ugal.ro

Cristina Marilena NIȚU
Institute of Solid Mechanics of the Romanian Academy, 15 Constantin Mille Str., 010141 Bucharest, Romania, cristina.nitu@imsar.ro

Abstract: - For certain categories of soils containing sand (15%), gravel (20%), clay (40%), stabilizers (15%) and water 10%, the appropriate rheological model for dynamic analysis is type E – (E/V). In this case, for the process of dynamic compaction on layers with thicknesses of 30÷50 cm, how is the analysis of the final effect required by assessing the degree of compaction.

This is achieved by the dynamic evaluation of the parameters in the resonance regime, the experimental and numerical results belonging to the authors are mentioned in the previously published papers [1].

Keywords: - Zener model; dynamic response; visco-elastic system.

1. INTRODUCTION

For the calibration tests of the compaction layers, testing grounds belonging to the Romanian road construction companies were used, where ICECON performed the experimental tests with the CV 10 machine produced by the Nicolina Iași company.

For the E – (E/V) model, the dynamic response in resonance was followed after each pass on the same layer. In the paper [10] with the same equipment and dynamic model evaluations were performed only in post-resonance, stable operation after the degree of compaction was calibrated in resonance. Thus, we specify that this article has the role of highlighting for the same model the correlation between the degree of compaction and the values of the resonance parameters as well as the modality of the changes after each pass on the same layer.

As a result of the experiments performed on the variety of harmonically excited linear viscoelastic materials, systems and structures, a dynamic behavior according to the Zener type rheological model was found.

The linear viscoelastic Zener system with the moving mass *m* has a rotating excitation inertial force, *F*(t), and the dynamic, transmitted reaction *Q*(t) depends on the model characteristics.

Dynamic response describes the evolution of the instantaneous displacement amplitude of the transmitted dynamic force and of the dissipated energy with respect to the continuous variation of the excitation pulsation $\Omega = \omega/\omega_n$ and depending on the discrete variation of the linear viscosity parameters ζ where ω_n is the natural pulsation of the system and ζ is the fraction of critical damping, such that $c = 2\zeta\omega_n m$.

Based on the families of curves drawn numerically and experimentally verified, the conclusions regarding the dynamic behavior of Zener modeled materials, systems and structures were established [1,2,3].

2. DETERMINATION OF AMPLITUDE AT RESONANCE

The dynamic model is presented in Figure 1, where $F = F(t) = F_0 \sin \omega t$, where either $F_0 = m_0 r \omega^2$, *c* is the linear viscous amortization proportional to the deformation speed of the viscous element, m is the mass, $k_1 = k$ rigidity of the Hooke elastic element, and $k_2 = kN$ is the rigidity of the elastic element in the structure of the Maxwell model, where *N* is a multiplication coefficient for rigidity k_1 [4,5].

The following experimental data have been used:

$m = 4 \cdot 10^3 kg; m_0 r = 20 kgm; k = 10^8 N/m; N = 10;$

$c = (7,9,11,13) \cdot 10^5 Ns/m; \zeta = 0,15; 0,18; 0,22; 0,32;$

$\omega = 0...500 rad/s; \Omega = 0...10.$

In complex wording, the movement differential equations are:

$$\begin{cases} m\ddot{\tilde{x}} + k_1\tilde{x}_1 - k_2\tilde{y} = F_0 e^{j\omega t} \\ c(\dot{\tilde{x}} - \dot{\tilde{y}}) = k_2\tilde{y} \end{cases} \quad (1)$$

The response in instantaneous displacement is given by the relations:

$$\tilde{x} = \tilde{X}e^{j\omega t}, \text{ unde } \tilde{X} = X_0 e^{j\varphi} \quad (2)$$

$$\tilde{y} = \tilde{Y}e^{j\omega t}, \text{ unde } \tilde{Y} = Y_0 e^{j\theta}$$

Introducing $\tilde{x}, \dot{\tilde{x}}, \ddot{\tilde{x}}$ and $\tilde{y}, \dot{\tilde{y}}$ in (1), we obtain the system in $\tilde{X}$ and $\tilde{Y}$, as follows:

$$\begin{cases} (k_1 - m\omega^2)\tilde{X} + k_2\tilde{Y} = F_0 \\ jc\omega\tilde{X} - (k_2 - jc\omega) = 0 \end{cases} \quad (3)$$

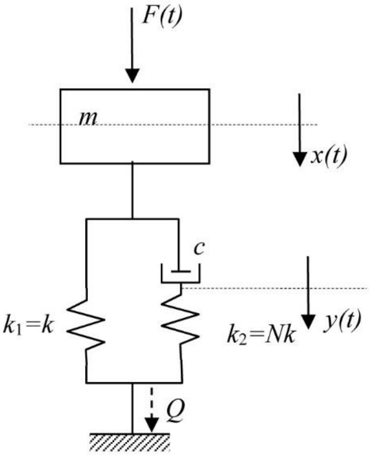

Figure 1. The linear harmonically excited Zener model

From (3) the amplitudes result:

$$X_0 = F_0\sqrt{\frac{k_2^2 + c^2\omega^2}{k_2^2(k_1 - m\omega^2)^2 + c^2\omega^2(k_1 + k_2 - m\omega^2)^2}} \quad (4)$$

$$Y_0 = F_0\frac{c\omega}{\sqrt{k_2^2(k_1 - m\omega^2)^2 + c^2\omega^2(k_1 + k_2 - m\omega^2)^2}} \quad (5)$$

The disadvantages φ and θ relative X_0 and Y_0 are as follows:

$$\tan\varphi = \frac{-c\omega k_2^2}{k_2^2(k_1 - m\omega^2)^2 + c^2\omega^2(k_1 + k_2 - m\omega^2)^2} \quad (6)$$

and

$$\tan\theta = -\frac{k_2(k_1 - m\omega^2)}{c\omega(k_1 + k_2 - m\omega^2)} \quad (7)$$

with relative sizes

$$\Omega = \frac{\omega}{\omega_n}, \qquad N = \frac{k_2}{k}$$

where $k = k_1 = m\omega_n^2, \zeta = c/(2m\omega_n), c\omega = (2\zeta\Omega)k$ the amplitudes X_0 and Y_0, based on Equations (9) and (10) may be expressed as:

$$X_0 = \frac{F_0}{k}\sqrt{\frac{N^2 + (2\zeta\Omega)^2}{N^2(1-\Omega^2)^2 + (2\zeta\Omega)^2(N+1-\Omega^2)^2}} \quad (8)$$

or

$$Y_0 = \frac{F_0}{k}\frac{2\zeta\Omega}{\sqrt{N^2(1-\Omega^2)^2 + (2\zeta\Omega)^2(N+1-\Omega^2)^2}} \quad (9)$$

Terms tan φ and tanθ, with relative sizes *Ω*, *N*, *ζ*, based on Equations (6) and (7), may be written as follows:

$$\tan\varphi = \frac{-2\zeta\Omega N^2}{N^2(1-\Omega^2)^2 + (2\zeta\Omega)^2(N+1-\Omega^2)^2} \quad (10)$$

or

$$\tan\theta = \frac{-(1-\Omega^2)N}{(2\zeta\Omega)(N+1-\Omega^2)} \quad (11)$$

The dynamic response to the excitation with force F(t) may be expressed by instantaneous displacements $x = x(t) = X_0\sin(\omega t + \varphi)$ and $y = y(t) = Y_0\sin(\omega t + \theta)$, where φ ϕ is the phase shift between *y(t)* and *F(t)*, and θ is the phase shift between *x(t)* and *F(t)*. In complex form, the dynamic response may be written as:

$$\begin{cases} \tilde{x} = \tilde{X}_0 e^{j(\omega + \varphi)} \\ \tilde{y} = \tilde{Y}_0 e^{j(\omega + \theta)} \end{cases} \quad (12)$$

which yields:

$$\begin{cases} x = Im\tilde{x} = X_0\sin(\omega t + \varphi) \\ y = Im\tilde{y} = Y_0\sin(\omega t + \theta) \end{cases} \quad (13)$$

Amplitudes X_0 and Y_0

a) Case of natural parameter sizes *ω, c, k_1, k_2.*

We introduce the amplitude of the excitation force in the Equations (4) and (5) as $F_0 = m_0 r\omega^2$.

For the continuous variation of the excitation pulsation ω and the discrete variation of the linear viscosity coefficient c, we have $X_0(c, \omega)$ and $Y_0(c, \omega)$ as:

$$X_0(c,\omega) = m_0 r\omega^2 \sqrt{\frac{N^2k^2 + c^2\omega^2}{N^2k^2(k-m\omega^2)^2 + c^2\omega^2(k+Nk-m\omega^2)^2}} \quad (14)$$

$$Y_0(c,\omega) = \frac{m_0 rc\omega^3}{\sqrt{N^2k^2(k-m\omega^2)^2 + c^2\omega^2(k+Nk-m\omega^2)^2}} \quad (15)$$

where X_0, Y_0 is in *m*, ω in rad/s, c in *Ns/m*.

b) Case with relative sizes **Ω, ζ, *N***

$$X_0(\zeta,\Omega) = \frac{m_0 r}{m}\Omega^2 \sqrt{\frac{N^2 + (2\zeta\Omega)^2}{N^2(1-\Omega^2)^2 + (2\zeta\Omega)^2(N+1-\Omega^2)^2}} \quad (16)$$

$$Y_0(\zeta,\Omega) = \frac{m_0 r}{m}\Omega^2 \frac{2\zeta\Omega}{\sqrt{N^2(1-\Omega^2)^2 + (2\zeta\Omega)^2(N+1-\Omega^2)^2}} \quad (17)$$

with representation in Figure 2 for $X_0(\zeta, \Omega)$ and in Figure 3 for $Y_0(\zeta, \Omega)$ for the force $F_0=(m_0 r)/mk\Omega^2$ [10].

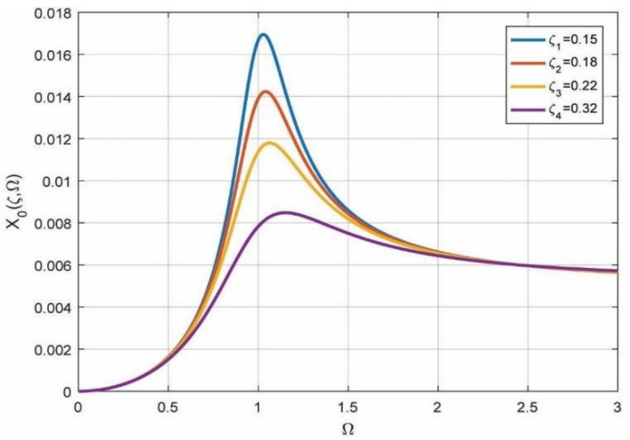

Figure 2. Plots of $X_0(\zeta, \Omega)$ for continuously varying Ω and discrete values of ζ.

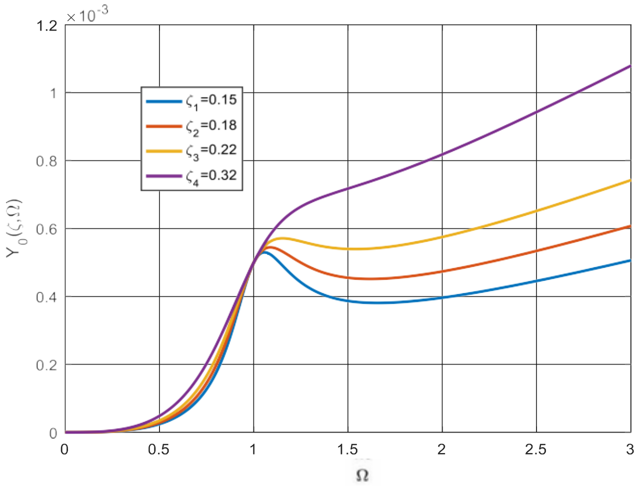

Figure 3. Plots of $Y_0(\zeta, \Omega)$ for continuously varying Ω and discrete values of ζ.

Amplitudes of $\bar{X}_0$ and $\bar{Y}_0$ at resonance

From the resonance condition for Ω=1, based on relations (16) and (17) it follows

$$\bar{X}_0 = \frac{m_0 r}{m}\sqrt{\frac{N^2 + 4\zeta^2}{4\zeta^2 N^2}} \quad (18)$$

$$\bar{Y}_0 = \frac{m_0 r}{m} \cdot \frac{1}{N} \quad (19)$$

Since $\zeta \le 0.5$ and $N \ge 10$ from (18) we have

$$\bar{X}_0 = \frac{m_0 r}{m} \cdot \frac{1}{\zeta N} \quad (20)$$

The degree of compaction with resonance calibration after runs is of the form

$$\bar{D} = \bar{D}_0\left(1 + \frac{\bar{X}_{0n}}{\bar{X}_{01}}\right) \quad (21)$$

where $\bar{D}_0$ is the degree of compaction at resonance after the first pass, i.e. at n=1

$\bar{X}_{0n}$ - amplitude at resonance after n passes

$\bar{X}_{01}$ - amplitude at resonance after the first pass

The ratio $\alpha_n = \frac{\bar{X}_{0n}}{\bar{X}_{01}}$ is of the form

$$\alpha_n = \frac{\zeta_n}{\zeta_1} \quad (22)$$

so that (21) becomes

$$\bar{D} = \bar{D}_0\left(1 + \frac{\zeta_n}{\zeta_1}\right) \quad (23)$$

In the case analyzed for $\bar{D}_0 = 32\%$, after 4 successive passes, at resonance, we have $\zeta_1 = 0,15$ and $\zeta_4 = 0,32$ which leads to reaching a degree of compaction with the value

$$\bar{D}_4 = 32\%\left(1 + \frac{0,32}{0,15}\right) = 100,26\%$$

3. DYNAMIC FORCE IMPARTED TO THE BASE AT RESONANCE

The force $\tilde{Q} = \tilde{Q}(t)$ transmitted to the fixed base in the complex, in the form

$$\tilde{Q} = \tilde{Q}(t) = k\tilde{x} + Nk\tilde{y} \quad (24)$$

where $k = k_1$, and $Nk = k_2$.

Introducing $\tilde{x}$ and $\tilde{y}$ as

$$\tilde{x} = \tilde{X}e^{j\omega t} = F_0 \frac{Nk + jc\omega}{\tilde{D}}$$

$$\tilde{y} = \tilde{Y}e^{j\omega t} = -F_0 \frac{jc\omega}{\tilde{D}}$$

in Equation (24), we obtain

$$\tilde{Q} = \frac{F_0}{\tilde{D}}[Nk^2 + jc\omega k(1+N)] \quad (25)$$

We introduce $\tilde{D} = Nk(k - m\omega^2) + jc\omega(k + Nk - m\omega^2)$ in Equation (25) and obtain:

$$\tilde{Q} = F_0 \frac{Nk^2 + jc\omega k(1+N)}{Nk(k - m\omega^2) + jc\omega(k + Nk - m\omega^2)} \quad (26)$$

We use the following notations, thus:

$$q_1 = Nk^2; q_2 = c\omega k(1+N); q_3 = Nk(k - m\omega^2);$$
$$q_4 = c\omega(k + Nk - m\omega^2)$$

The relation (26) can be expressed as

$$\tilde{Q} = F_0 \frac{q_1 + jq_2}{q_3 + jq_4}$$

whence the amplitude Q_0^2 follows thus:

$$\left|\tilde{Q}\right|^2 = Q_0^2 = F_0^2 \frac{q_1^2 + q_2^2}{q_3^2 + q_4^2}$$

from where the amplitude of the transmitted force Q_0 can be formulated as:

$$Q_0 = F_0 \sqrt{\frac{q_1^2 + q_2^2}{q_3^2 + q_4^2}} \quad (27)$$

Replacing $q_1; q_2; q_3; q_4$ with prior notations, we obtain Q_0 in natural sizes, as follows:

$$Q_0(c,\omega) = F_0 \sqrt{\frac{N^2k^4 + c^2\omega^2k^2(1+N)^2}{N^2k^2(k - m\omega^2)^2 + c^2\omega^2(k + Nk - m\omega^2)^2}} \quad (28)$$

In the relative parameters Ω, ζ, and N, Equation (29) may be written as:

$$Q_0(\zeta,\Omega) = F_0 \sqrt{\frac{N^2 + (2\zeta\Omega)^2(1+N)^2}{N^2(1-\Omega^2)^2 + (2\zeta\Omega)^2(N+1-\Omega^2)^2}} \quad (29)$$

(a) Case of natural sizes

$$Q_0(c,m) = m_0 r\omega^2 \cdot R(c,\omega)$$

where R(c, ω) is given by the relation

$$R(c,\omega) = \sqrt{\frac{N^2k^4 + c^2\omega^2k^2(1+N)^2}{N^2k^2(k - m\omega^2)^2 + c^2\omega^2(k + Nk - m\omega^2)^2}} \quad (30)$$

(b) Case of relative sizes

$$Q_0(\zeta,\Omega) = \frac{m_0 r}{m} k\Omega^2 \cdot R(\zeta,\Omega)$$

where R(ζ, Ω) is given by the relation

$$R(\zeta,\Omega) = \sqrt{\frac{N^2 + (2\zeta\Omega)^2(1+N)^2}{N^2(1-\Omega^2)^2 + (2\zeta\Omega)^2(N+1-\Omega^2)^2}} \quad (31)$$

where $F_0 = m_0 r\omega^2$, depending on ω and respectively $F_0 = (m_0 r)/mk\Omega^2$ depending on $\Omega = \omega/\omega_n$, represented in figure 4 [7].

$$\bar{Q}_0 = \frac{m_0 r}{m} k \sqrt{\frac{N^2 + 4\zeta^2(1+N)^2}{4\zeta^2 N^2}} \quad (32)$$

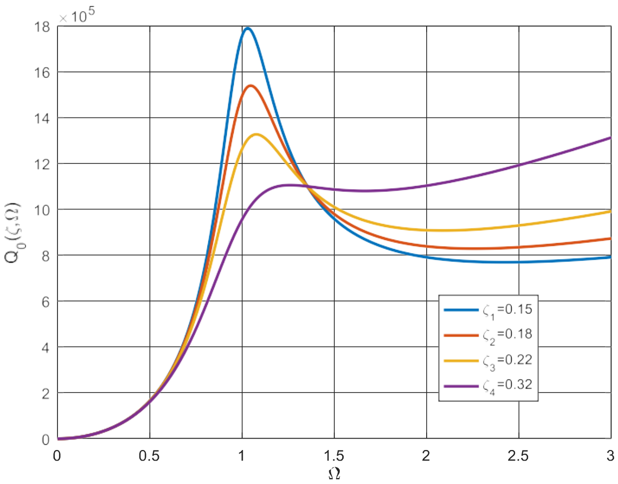

Figure 4. Plots of transmitted force amplitude $Q_0(\zeta, \Omega)$ excitation force $F_0 = (m_0 r)/m\ k\Omega^2$

4. CONCLUSIONS

Numerical analysis and experimental data allowed for the adjustment of a Zener rheological model, with mass and harmonic excitation using inertial rotating force.

Establishing calculation relations and parametric graphic representation with identification of dynamic regimes. Thus, based on the calculation relationships and the parametric evaluation, the following conclusions can be synthesized [8,9]:

a) the X_0 and Y_0 amplitudes define the largest displacements of the mass *m*, and, respectively, of the elastic component $k_2 = kN$, which is useful in the evaluation of the technological parameters;

b) the parametric curves of amplitudes X_0 and Y_0 show distributions depending on the ante-resonance, resonance, and post-resonance dynamic regimes;

c) the dynamic area of interest for the stable behavior of technological vibrations is specific to the post-resonance field.

Thus, for significantly high values of the excitation pulsations, in conditions of predictable amortization, the X_0 amplitude presents a stable layer at low variations of the excitation pulsation, suggesting that Y_0 continuously increased with ω.

d) the maximal dynamic transmitted force Q_0 in the post-resonance field for $\omega >> \omega_n$ or $\Omega >> 1$, shows the stable values set by the size of the viscous amortization;

e) the degree of compaction is established for the values of the parameters at resonance.

Based on the physical–mechanical parameters specific to the Zener rheological model for viscoelastic materials, systems, and structures, assessments can be performed on the parameter sizes of the dynamic answer and behavior in the harmonic excitation regime with harmonic rotation forces.

REFERENCES

[1] Bratu, P.; Dobrescu, C. Dynamic Response of Zener-Modelled Linearly Viscoelastic Systems under Harmonic Excitation, *Symmetry*, 2019, 11, 1050. https://doi.org/10.3390/sym11081050

[2] Drăgan, N., Potîrniche, A.M. And Căpățână, G.F. 2022. Effect of Reducing the Vibrations Transmitted with High-Performance Elastomeric Devices, *Romanian Journal of Acoustics and Vibration*, vol. 18, 2 (Feb. 2022), 126-129.

[3] Drăgan, N., A numerical approach of power analysis for the elastical mechanical systems with nonlinear damping, *Romanian Journal of Acoustics and Vibration*, Vol. 5, No. 1, Ed. Impuls, ISSN 1584-7284, Bucharest, 2008

[4] Polidor, B., Stuparu, A., Popa, S., Voicu, O., Iacob, N., Spânu, G. The dynamic isolation performances analysis of the vibrating equipment with elastic links to a fixed base. vol. 61, no. 1 (2018): *ACTA Technica Napocensis - Applied Mathematics, mechanics and engineering*.

[5] Morariu-Gligor, R., Crișan, A., Șerdean, F. Optimal design of an one-way plate compactor. Vol. 60, No. 4 (2017): *ACTA Technica Napocensis - applied mathematics, mechanics and engineering*.

[6] Nastac, S., Debeleac, C., Nechita, P. Assessments on shock absorption properties of foam-formed low density cellulose composites. Vol. 60, No. 4 (2017): *ACTA Technica Napocensis - applied mathematics, mechanics and engineering*.

[7] Morariu-Gligor, R.M. Factors influencing the degree of soil compaction. Vol. 60, No. 1 (2017): *ACTA Technica Napocensis - Series: Applied mathematics and mechanics*.

[8] Potîrniche, A., Năstac, S. Functional correlations regarding passive isolation of symmetrical systems. Vol. 56, No. 4 (2013): *ACTA Technica Napocensis - Series: Applied mathematics, mechanics and engineering*.

[9] Vasile, O., Vlase, S., Năstac, C., Scutaru, M.L. Experimental analysis of a mechanical system composed by two identical parts. Vol. 61, No. 3 (2018): *ACTA Technica Napocensis - applied mathematics, mechanics and engineering.*